energy&fuels

Article

pubs.acs.org/EF

Pyrolysis of Potassium-Doped Wood at the Centimeter and Submillimeter Scales

Mishal H. Shah,[†,‡] Lei Deng,[§,‡] Hayat Bennadji,[‡,∥] and Elizabeth M. Fisher*[,‡]

[†]Department of Chemical Engineering, Loughborough University, Loughborough, Leicestershire LE11 3TU, United Kingdom
[‡]Sibley School of Mechanical and Aerospace Engineering, Cornell University, Ithaca, New York 14853, United States
[§]School of Energy and Power Engineering, Xi'an Jiaotong University, Xi'an 710049, China

Supporting Information

ABSTRACT: The effect of potassium additives on pyrolysis of poplar was investigated at 427 °C, both at the submillimeter scale, through thermogravimetric analysis (TGA), and at the centimeter scale, through pyrolysis of wood cylinders in a turbulent reactor. Internal temperatures and time-resolved rates of production of gases and light volatiles were measured in the centimeter-scale study. The potassium level in the samples was varied through vacuum treatment with distilled water or solutions of KCl or K_2CO_3, resulting in potassium levels of approximately 100, 4500, and 7000 ppm (dry, mass basis). At the centimeter scale, potassium addition had a dramatic effect on conversion time and on the magnitude of exothermic temperature excursions, as well as a significant effect on the yields of gases and light volatiles. Consistent with the literature, submillimeter-scale TGA experiments with external temperature control also indicated a catalytic effect of the potassium additives, with K_2CO_3 more effective than KCl in promoting pyrolysis and char formation.

INTRODUCTION

Experiments at the submillimeter scale have shown that mineral content of biomass has a strong effect on the pyrolysis process and thus on the thermochemical conversion of biomass to heat, useful energy carriers, and/or other useful products. Thermal conversion processes start with the pyrolysis or devolatilization of biomass, producing a range of gaseous, condensable, and solid products, which are known generically as gas, tar, and char. The proportions, conversion rates, and detailed composition of these product streams depend on many operational variables and biomass characteristics including mineral content.

Alkali metals, especially potassium, are among the most abundant of inorganics present in biomass.[1] Potassium levels in biomass vary over a wide range depending on biomass type and growing conditions;[1] for example, Baxter et al.[2] report potassium mass fractions of 0.4% in wood-derived fuels, 2% in straws, and 3% in almond hulls; 80−90% of this potassium is in water-soluble or ion exchangeable forms. The literature indicates that higher potassium levels in biomass are generally associated with lower temperatures required for pyrolysis, lower levels of tars, and higher levels of gases and chars in the product stream,[3−7] Although slow pyrolysis experiments follow these trends, some fast pyrolysis experiments show different behavior.[8−10] The impact of potassium on the yields of specific products and classes of products has also been documented.[3,10−15] Catalytic effects of potassium have been demonstrated at levels as low as 0.05% potassium by mass.[15]

Numerous studies have compared low- and high-potassium versions of the same powdered biomass material, in order to isolate the potassium effects. In some of these studies, differences in potassium loading are achieved through washing away naturally occurring potassium, using acid or hot water.[3,8,16−18] In others, higher levels of potassium are achieved by mechanically mixing potassium salts with powdered biomass,[19] by soaking biomass powder in potassium salt solutions,[16] or by multistep ion-exchange processes.[20] With a few exceptions,[8] the effect of potassium addition or removal on pyrolysis is investigated using submillimeter-scale biomass particles, either in fluidized beds[9] or in thermogravimetric measurements where the temperature of submillimeter-scale biomass particles is externally controlled during slow heating.[3,21] Although these experiments are useful, they do not provide information about the influence of thermochemistry and intraparticle secondary charring reactions.

The current study takes a different approach to doping biomass that makes it possible to adjust potassium content in centimeter-scale biomass samples. Thus, we are able to pyrolyze low- and high-potassium biomass samples at the centimeter scale, altering the pyrolysis kinetics while having a minimal impact on heat-transfer characteristics. The centimeter and larger scale is important in devices such as fixed bed gasifiers and has proven useful for elucidating the effects of thermochemistry.[21] Although the impact of potassium on kinetics should remain the same as in submillimeter experiments, the importance of the kinetics may be substantially reduced in the case of heat-transfer-limited pyrolysis in larger particles.

The relative speeds of chemical kinetics, internal heat transfer, and external heat transfer are typically described in terms of the Pyrolysis and Biot numbers, Py and Bi.[22,23] Under the conditions tested, the Biot number is approximately 5, indicating a thermally thick condition with significant internal temperature gradients. The Pyrolysis number, based on

Received: August 4, 2015
Revised: October 12, 2015
Published: October 15, 2015

DOI: 10.1021/acs.energyfuels.5b01776
Energy Fuels 2015, 29, 7350−7357

Table 1. Mass Loading of Potassium in Wood Samples, Dry Basis, Determined with Different Methods

doping liquid	ppm K, based on wet vs dry cylinder mass during doping[a]	ppm K, based on change in dry cylinder mass before and after doping[a]	ppm K, based on ICP measurements, average of spatially resolved measurements	ppm K, based on ICP measurements of samples used for TGA
distilled H_2O	N/A	N/A	180	129
0.900% aqueous solution KCl (low KCl)	6300 ± 280	5780 ± 350 if added mass is KCl	4640	4700
1.560% aqueous solution KCl (high KCl)	11540 ± 160	9390 ± 260 if added mass is KCl	6940	7600
1.444% aqueous solution K_2CO_3	10770 ± 300	9230 ± 470 if added mass is K_2O	7220	8380

[a]Note: ± values represent standard deviations over the 5−7 cylinders used in the experiments.

cellulose kinetics[22] at the final temperature, is below 0.01, indicating that the conversion time should be determined by the heat-transfer process, which is much slower than the chemical kinetics. Thus, on the basis of the value of Py, we would anticipate the catalytic effect of the potassium on kinetics to have minimal impact on conversion times. The results of the current study, which contradict these expectations, indicate some problems with using the Pyrolysis number to characterize the behavior of large particles.

MATERIALS, APPARATUS, AND METHODS

Chemicals and Preparation of Wood Samples. Potassium chloride (purity ≥99.5%) and potassium carbonate (purity ≥99%), were purchased from Sigma-Aldrich, St. Louis, MO and were used to prepare solutions with distilled water; mass fractions are given in Table 1. A single dowel of dried, untreated poplar, free from visible knots and heartwood, was purchased from Lowes Home Improvement, Ithaca, NY. The dowel was cut into cylinders of the specified length and dried to completion at 105 °C in air. Next, in sets of seven, the cylinders were treated with either distilled water or salt solutions, as follows. The cylinders were immersed in 2.5 L of the water or solution and held below the liquid surface with weights. The pressure in the container was lowered to 2450 Pa with a vacuum pump, and that pressure was maintained for 5 h (i.e., until bubbles had essentially stopped emerging from the wood). The treated cylinders were then dried in air in a process developed by trial and error as a trade-off between cracking/splitting (at high drying rates) and mold growth (at low drying rates). For the first 90−140 h, the cylinders were stored on end in a small beaker inside a desiccator. Approximately once a day, the cylinder orientation was reversed and fresh Drierite desiccant was placed in the desiccator. During this stage, the cylinders lost approximately 8.4% of the added water mass per day. Upon first appearance of tiny dots of mold, the cylinders were transferred to an oven and dried at 40 °C for 24 h, subsequently, they were dried at 105 °C to completion. All drying took place in air. No visible cracking or splitting occurred with this drying regimen. Treated cylinders were stored in a desiccator until used.

Analysis of Mineral Content. Samples were prepared for mineral analysis as follows: a cylinder was held in a lathe, and specific sections of it were cut into shavings with a cutting tool or drill bit. All surfaces in contact with the wood had been cleaned with alcohol and dried before use, and the shavings were collected on fresh aluminum foil.

Dry shavings (mass 0.14 to 1.5 g) were weighed and then digested with nitric and perchloric acid in an automated Vulcan 84 digestion unit (Questron Technologies, Mississauga Canada). Digestion took place over the course of 3 h, with a controlled temperature program with a maximum temperature of 180 °C. Yttrium was added to the mixture before digestion, for use as an internal standard. The solutions were analyzed for their elemental composition by inductively coupled plasma atomic emissions spectroscopy (ICP-AES) using an axial viewed Spectro Arcos ICP-AES (Kleve, Germany).

ICP measurements of potassium and other minerals were performed for two different cylinders treated with each doping treatment and reported on a dry basis. For the first cylinder, spatially resolved ICP readings were obtained by analyzing shavings from different regions of the cylinder. Averages for the entire cylinder were then obtained by averaging the spatially resolved results, weighted by the volume of the sampled region. For the second cylinder, the ICP measurements were performed on a powder obtained by converting the entire cylinder to shavings, which were then ball-milled and sieved.

Submillimeter-Scale Pyrolysis Experiments. Wood shavings from an entire cylinder were converted to powder using a ball mill, then sieved to retain particles below 250 μm. Experiments were performed in duplicate with sample masses between 6.4 and 14.2 mg, using platinum crucibles in a TA Instruments (New Castle, DE) Q500 thermogravimetric analyzer (TGA). The temperature profile was the following: 20 °C/min to 105 °C; hold at 105 °C for 10 min; 5 °C/min to 416 °C; hold at 416 °C for 10 min. Sample and balance purge flows were N_2 with flow rates of 60 and 40 standard cubic centimeters per minute, respectively. Masses were referenced to the mass at the end of the 105 °C plateau (i.e., presented on a dry basis). The rate of change of mass was determined without smoothing, using first-order forward differencing.

Centimeter-Scale Pyrolysis Experiments. Each wood cylinder was pyrolyzed individually by insertion into a turbulent nitrogen flow that had been preheated to 427 °C. Details of the pyrolysis method and measurement techniques are described elsewhere;[24] key features are outlined here. During pyrolysis, temperatures at two locations inside the wood were monitored with 0.5 mm-OD sheathed type K thermocouples. Products were sampled continuously through the gas cell of an online FTIR system, which was used to quantify gaseous and light volatile products. An NDIR system was also used to quantify carbon monoxide with better time resolution. After pyrolysis, the cylinder was withdrawn into an unheated side arm of the reactor and cooled with a cold nitrogen flow until its temperature dropped below 100 °C, when it was removed and placed in a desiccator. The choice of reactor temperature and the unusual reactor design produce initial heat fluxes on the order of 20 W/m^2, with rapid dilution and no extra-particle reaction of product gases. The apparatus, procedure, and operating conditions, including nitrogen and sampling flow rates, were as described previously[24] with the following exceptions: (1) the cylinder was held in the high-temperature flow for only 20 min; (2) turbulizers had been added to the reactor upstream of the wood insertion point; and 3) thermocouple positions in the wood were different, and a third thermocouple monitored the gas temperature near the wood, providing an accurate indication of the time of insertion.

RESULTS AND DISCUSSION

Wood and Cylinder Characteristics. At the end of the entire treatment process, the cylinders' diameters were 1.889 ± 0.009 cm, and their lengths were 4.010 ± 0.001 cm, essentially unchanged from the start of the treatment. The density of the wood after washing with distilled water and drying was 523.8 kg/m^3, and the mass fractions C, H, O, and N of the water-treated wood were 54.9%, 6.21%, and 46.4%, and 0.09%,

DOI: 10.1021/acs.energyfuels.5b01776
Energy Fuels 2015, 29, 7350−7357

respectively, on a dry basis, as determined with an NC2500 elemental analyzer. The porosity of the wood, ε, was estimated from m_{dry} and m_{wet}, the mass measured immediately before and after soaking in water or salt solution, respectively:

$$\varepsilon = \frac{m_{wet} - m_{dry}}{\rho_{liquid} V_{cylinder}}$$

This value obtained, 71%, agrees reasonably well with the value obtained from the measured dry density and the theoretical density of void-free wood,[25] which was 65%.

Potassium Loading: Average and Spatial Distribution. Average potassium levels in the doped wood were determined in several different ways, giving generally consistent results, as seen in Table 1. First, potassium levels were estimated by comparing the dry mass before doping to the wet mass of the cylinder immediately after doping, and assuming that the mass of liquid added to the cylinder had the same composition as the initial aqueous solution. Next, masses of the dried treated cylinders were compared to the dry masses before doping, and K fraction was calculated on the assumption that the mass added to the cylinder was either KCl or K_2O. Note that treating the cylinders with distilled water resulted in minimal net change in mass (loss of 0.04% of the initial mass). Lastly, the mineral mass fractions of K and other minerals were analyzed by ICP for selected cylinders, as described above.

In all cases, the average concentration of potassium was similar in the K_2CO_3 and high-KCl samples and was approximately 40% lower in the low-KCl samples, consistent with the potassium concentrations of the solutions used in preparing the samples. The potassium levels achieved were comparable to those in high-mineral biomass. Note that the change in dry cylinder mass gives consistent results only when it is assumed that the K_2CO_3-doped samples lost the added CO_2 during the drying process. Although dilute K_2CO_3 solutions absorb CO_2 from the gas phase,[26] the process can shift to desorption as evaporation proceeds and produces more concentrated solutions.

Potassium content of the untreated poplar wood was not measured, but the levels of potassium in the distilled-water cases are reduced approximately 10-fold from typical literature values for hardwoods.[27] However, because of mass-transfer limitations in the wood cylinders, the distilled water treatment did not remove minerals to the very low levels typically achieved in washing of powdered biomass (typically 2−40 ppm).[13] Note that the mass fractions of other minerals are listed in the Suppporting Information.

A representative spatial distribution of potassium (measured for a K_2CO_3-doped cylinder) is shown in Figure 1, with the width of the symbol representing the axial extent of the spatial region (annulus or cylinder of equal volume) from which the shavings were made. Note that spatially resolved data is not available in one axial region, which was used for holding the sample in the lathe. The spatial distribution of the potassium is highly nonuniform, with much higher levels near the surfaces where the drying occurred, namely, at the axial positions closest to the upper end of the cylinder, and at the radially outer positions. Similar results have been observed by Smith and Cockcroft,[28] and appear to be due to the transport of salt-laden liquid during the drying process. In the future, if a more uniform loading is desired, larger wood cylinders could be doped and dried, then machined down to remove the outer region where most of the spatial variability occurs. Spatial

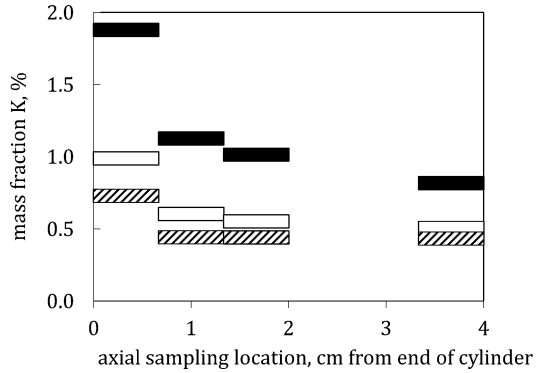

Figure 1. Spatial distribution of potassium in a wood cylinder doped with K_2CO_3. Each measurement is an average over an equal volume of wood. Different shadings represent different radial positions. For black, $(2R/3)^{1/2} \le r \le R$; for white, $(R/3)^{1/2} \le r \le (2R/3)^{1/2}$; for striped, $r \le (R/3)^{1/}$, where R is the cylinder radius and r is the sampling radius.

distributions for the other cylinders show similar patterns. Even in the distilled-water case, naturally occurring potassium was redistributed during drying to create a similar spatial pattern.

Submillimeter-Scale Pyrolysis Experiments. Figure 2 shows the results of TGA experiments. For each wood

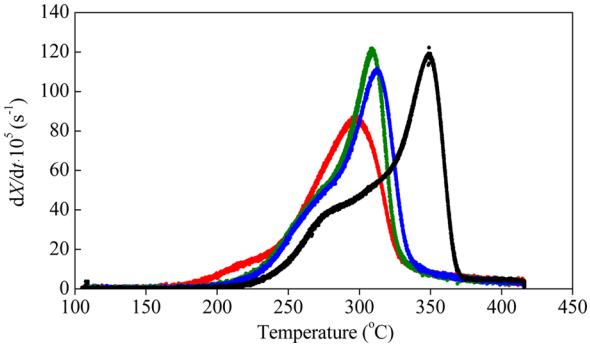

Figure 2. Rate of change of mass normalized by dry mass, versus temperature, from thermogravimetric analyzer experiments for four different wood treatments: black: distilled water; blue: low KCl; green: high KCl; red: K_2CO_3.

treatment, results from two runs are overlaid in the same color. The duplicate TGA results are virtually indistinguishable on the scale of the figure. This agreement, despite large differences in initial sample mass (e.g., 12 vs 6.4 mg), indicates that the sample was under kinetic control during pyrolysis. If mass-transfer limitations had been important, then results with different sample masses would have differed significantly.

Figure 2 shows a substantial impact of the potassium treatment on the pyrolysis kinetics, as observed previously. The water-treated wood shows typical behavior, with a maximum at 349 °C, and a shoulder around 275 °C, consistent with the decomposition of cellulose and hemicellulose.[7] The wood treated with high and low KCl concentrations shows qualitatively similar behavior but with all features shifted to lower temperatures. The shift of the cellulose peak, to 309 and 312 °C for the two treatments, is greater than the shift of the shoulder, to about 260 °C. The K_2CO_3-treated wood pyrolyzes at an even lower temperature, with its peak rate of mass loss occurring at 297 °C. For this treatment, it appears that the hemicellulose and cellulose peaks have merged; however, a small shoulder is visible at about 220 °C. Char levels measured

DOI: 10.1021/acs.energyfuels.5b01776
Energy Fuels 2015, 29, 7350−7357

at the end of the pyrolysis process at 416 °C are 14.3%, 24.0%, 25.3%, and 27.2%, on a dry basis, respectively, for wood treated with distilled water, low KCl, high KCl, and K_2CO_3.

The TGA results are consistent with the literature. The peak decomposition temperature is 10−15 °C lower in the water-treated samples of the current study than in the water-washed hardwood samples of Mueller Hagedorn et al.[13] at the same heating rate. This difference may be due to the somewhat higher K levels in the water-treated samples than in Mueller-Hagedorn's washed biomass,[7] or it may simply reflect differences in the starting biomass composition. Consistent with the present study, Mueller-Hagedorn[13] observed substantial reductions in the temperature of peak decomposition with potassium doping of 5000 ppm. Also consistent with the current study are previous observations[29] that catalytic effects are not sensitive to the differences in potassium loading level in the range 4000−54 000 ppm.

Other researchers have specifically examined KCl and K_2CO_3 additives, and the differences in their effects on pyrolysis. At mass fractions similar to those in the present study, Liu et al.[30] found that both KCl and K_2CO_3 decreased the temperature at which pyrolysis of cellulose occurred, and both promoted the formation of char. K_2CO_3 was somewhat more effective catalytically than the same K loading of KCl. Yang et al.[31,32] investigated the effect of minerals on pyrolysis of biomass components (cellulose, hemicellulose, and lignin), mixtures of components, and biomass. Different mineral additives, including KCl and K_2CO_3, were mixed directly with the components at very high loadings (10% by mass), and thermogravimetric analysis was performed. Neither KCl nor K_2CO_3 influenced lignin pyrolysis behavior in the temperature range of the present study. For K_2CO_3, there was a promoting effect on cellulose pyrolysis and an inhibiting effect on hemicellulose pyrolysis, in both cases producing a DTG trace that seemed to show two decomposition processes occurring at different temperature ranges. KCl had little effect on the temperature of peak decomposition, but it reduced the peak mass loss rate, thus producing more char. In contrast, Raveendran et al.[4] reported only a small impact of the anion on char yields for washed biomass samples impregnated with different potassium salts. Di Blasi et al.[14] investigated the effects of added NaOH, NaCl, K_2CO_3, and other alkali salts on the pyrolysis of washed fir wood. They found, as in the current study, that the additives with the lower pH tended to have a greater catalytic effect on pyrolysis.

Centimeter-Scale Pyrolysis Experiments. Figure 3 shows typical temperature histories at the center of the wood cylinder. Each different line corresponds to a different wood cylinder pyrolysis experiment, with green lines corresponding to doping with the high-KCl solution and black lines corresponding to water treatment. The run-to-run differences among green lines or among black lines are due to (1) small differences in the placement of the thermocouple tip, and (2) continuing small changes in temperature of heated gases and reactor walls even after the system's 4 h warm-up time. In the case of the KCl-doped experiments, two of the runs also show abrupt changes in the slope of the temperature history (around 220 s after insertion). These changes are apparently due to splitting of the wood and the exposure of the thermocouple to direct heat transfer to the turbulent nitrogen flow. Upon removal from the reactor, runs with abrupt slope changes were found to have split char samples and/or missing parts of the char. When splitting occurred, it invariably exposed a

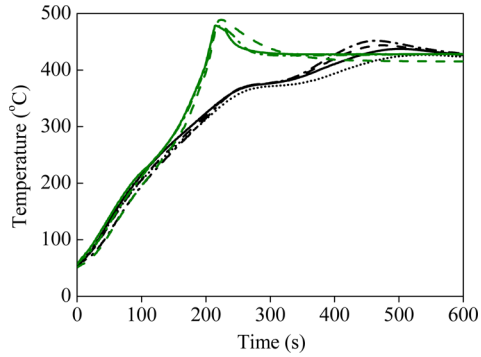

Figure 3. Representative centerline temperature traces. Each curve is a separate experiment; different colors correspond to different wood treatments: black: distilled water; green: high KCl.

thermocouple. Temperature plots in Figure 4 show average temperature histories for a given treatment and thermocouple

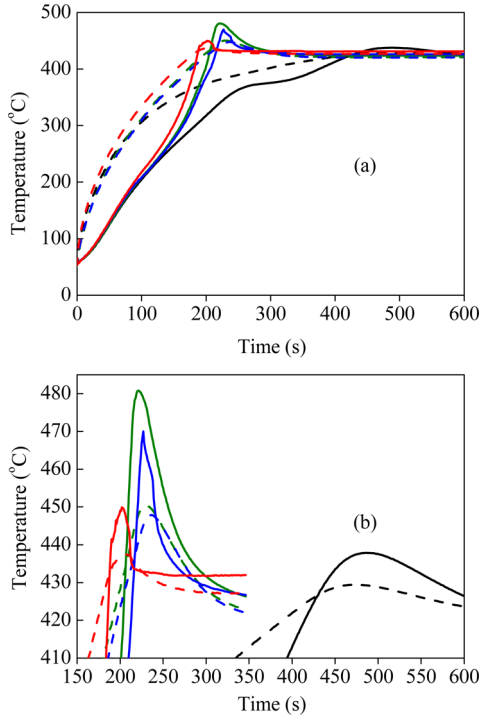

Figure 4. Temperature profiles at the center (solid lines) and at $R/2$, $L/4$ (dashed line) for four different wood treatments: black: distilled water; blue: low KCl; green: high KCl; red: K_2CO_3. Each line is the average of results from 3 or 4 experiments. Part (b) is a closeup view, with temperatures plotted only in the vicinity of the temperature peak for each treatment.

location. In that figure, solid lines are measured at the center of the cylinder, while dotted lines are measured at $L/4$, $R/2$. The jagged appearance of the centerline temperature history for K_2CO_3-doped and high-KCl-doped wood appear to be due to wood splitting.

As previously observed for undoped wood samples,[21,24,33,34] the temperature histories show complex behavior because of the interaction between (1) heating by the nitrogen flow and walls of the reactor, which tends to bring the sample to thermal equilibrium with the external gas, and (2) endo- and exothermic reactions within the pyrolyzing wood. Because external heating is less important at the center of the particle,

DOI: 10.1021/acs.energyfuels.5b01776
Energy Fuels 2015, 29, 7350−7357

the center temperature histories show the greatest extremes of slope. Similarly, the faster pyrolysis of the doped wood samples allows less time for heat transfer; thus, these samples are further from thermal equilibrium with the outside gas temperature and show greater effects of reaction thermochemistry.

Figure 4 shows that samples with all four wood treatments have very similar temperature histories at temperatures below about 200 °C (i.e., before reactions become significant). This similar low-temperature behavior implies that the potassium additives have minimal effect on the heat transfer properties of the samples. Above 200 °C, the temperature histories start diverging: first the K_2CO_3-doped sample rises more rapidly than the other three, then, at a slightly higher temperature, the two KCl-doped samples separate from the water-treated sample. All four samples show inflection points and maxima, but the locations of the maxima are affected by cracking/splitting in the K_2CO_3-doped and high-KCl-doped samples. The maxima of the three potassium-doped cases occur more than two times sooner than the maximum of the water-treated sample; the kinetics is fastest for K_2CO_3-doping, then high-KCl, then low-KCl. The timing of the temperature maximum is similar for the thermocouple at $R/2$, $L/4$ and the center thermocouple.

Following the analysis of Di Blasi et al.,[21] it is interesting to examine the time derivative of the center temperature, or "heating rate", in Figure 5. After reactions start around 100 s,

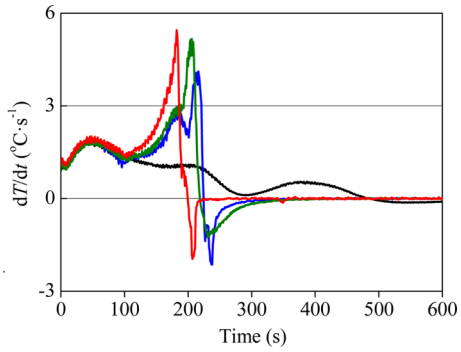

Figure 5. Rate of temperature increase with time, center of particle, for four different wood treatments: black: distilled water; blue: low KCl; green: high KCl; red: K_2CO_3. Each line is the average of results from 3 or 4 experiments. Temperatures are smoothed (moving average) and then numerically differentiated.

the time derivative of temperature shows somewhat different behavior for the four different wood treatments. For water-treated and low-KCl-doped samples, there are two peaks separated by a minimum, the same pattern observed by Di Blasi and co-workers for undoped samples of beech wood.[21] For the high-KCl-doped sample, the two peaks start to merge into a peak and a shoulder, and for the K_2CO_3-doped sample, there is a single peak, cut short by splitting of the sample. Although the timing of the peaks and minimum are different for the different samples, the temperatures at which these features occur are comparable for the different treatments, and also compatible with the observations of Di Blasi and co-workers for undoped wood.[21] The two peaks, occurring at approximately 320−330 °C and 400−425 °C, are attributed to exothermic decomposition of hemicellulose and lignin, respectively.[21] The minimum in heating rate is attributed to the combined effect of endothermic decomposition of lignin and cellulose.[21] The merging of these processes in the heating rate profiles reflects the merging of the mass loss peaks in the TGA profiles (Figure 2), as the catalytic effects of the potassium addition become stronger. Note that the initial heat flux estimated for the current experiments, 22 kW/m^2, is comparable to that experienced in the Di Blasi et al.[21] experiments.

Potassium addition has a strong effect on the generation of gases and volatiles. Figures 6−9 show the time histories of the

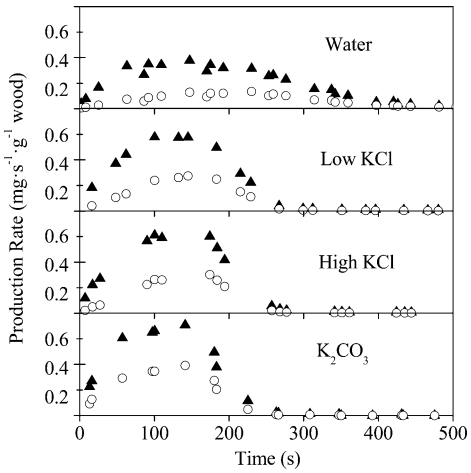

Figure 6. Rate of production of carbon dioxide (triangles) and carbon monoxide (circles), versus time after insertion, for four different wood treatments, on a dry additive-free basis. Results from three or more experiments for each treatment are plotted together.

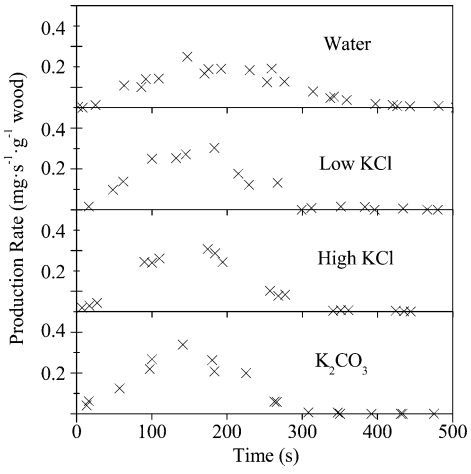

Figure 7. Rate of production of acetic acid versus time after insertion, for four different wood treatments, on a dry additive-free basis. Results from three or more experiments for each treatment are plotted together.

rates of generation of the species measured by FTIR. Each plot shows data from multiple samples, generally with very good consistency from sample to sample. The potassium additives affect both the timing of gas generation (much shorter for K-doped samples) and the composition of the gas mixture. A consistent progression from water-treated, to KCl-treated, and finally to K_2CO_3-treated samples, is observed for most species. The two different loadings of KCl produce essentially indistinguishable species histories, as can be seen by plotting them together (not shown here).

Table 2 lists integrated yields on a dry, additive-free basis. Potassium addition is associated with higher char and gas yields.

DOI: 10.1021/acs.energyfuels.5b01776
Energy Fuels 2015, 29, 7350−7357

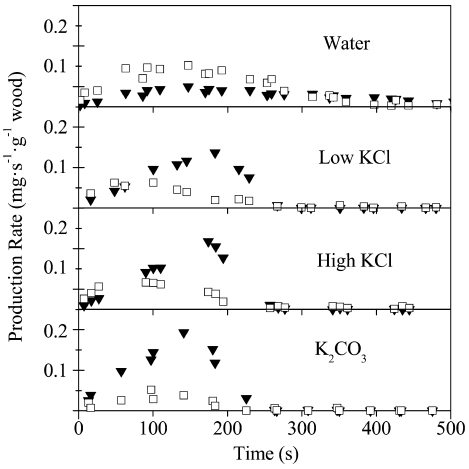

Figure 8. Rate of production of methanol (triangles) and formaldehyde (squares) versus time after insertion, for four different wood treatments, on a dry additive-free basis. Results from three or more experiments for each treatment are plotted together.

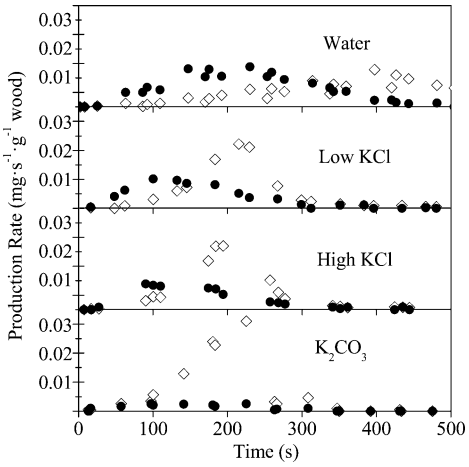

Figure 9. Rate of production of methane (diamonds) and formic acid (circles) versus time after insertion, for four different wood treatments, on a dry additive-free basis. Results from three or more experiments for each treatment are plotted together.

For a given wood treatment, char yields are also higher than seen in the corresponding TGA cases, probably reflecting the occurrence of secondary charring reactions in the centimeter-scale samples. For most species, yields for the two KCl-doped samples are very similar to each other. Generally, the water-doped samples have one extreme of yields and the K_2CO_3-doped samples have the opposite extreme. Yields of CO_2, CO, and methanol increase as potassium is added, while yields of formic acid and formaldehyde decrease. Changes in yields with additive loading may be due to additives' effects on temperature histories and secondary tar reactions,[35] as well as their effect on pyrolysis kinetics. Because methanol, CO, and CO_2 yields increase with temperature in the current range of conditions,[36] their increased yields with K may actually be due to the higher maximum temperatures encountered in doped samples. Because formic acid yields decrease with temperature and also with particle size,[36] its decreased yield with K addition may be due to secondary reactions or to higher peak temperature. It is impossible to separate out the effects of these three modes of action with the information available. However, the timing of

Table 2. Yields of All Measured Species and Char, mg/kg, Dry, Additive-Free Basis[a]

	distilled water	KCl, low	KCl, high	K_2CO_3
gases:				
carbon dioxide	102.6	108.2	110.5	116.1
carbon monoxide	36.3	45.1	46.8	59.6
methane	3.3	2.7	2.8	3.4
sum of gases	142.2	156.0	160.1	179.1
tars:				
acetic acid	47.0	51.5	54.9	52.4
formaldehyde	24.6	10.5	11.7	5.8
methanol	14.7	21.1	22.6	26.0
formic acid	3.2	1.8	1.6	0.5
char	249.5 ± 4.3	290.5 ± 1.7	288.9 ± 2.7	n.m.

[a]Gas and tar yields were obtained through a trapezoid rule integral of the FTIR species data, combining multiple runs. For the char, the standard deviation of repeated measurements is reported. Char yield was not measured for the case marked "n.m." because parts of the char broke off in the reactor and were not retrieved. The measured mass of potassium additive is subtracted from the measured solid mass to obtain the char mass for use in this table.

the appearance of CH_4 (coincident with the brief high-temperature excursion) supports attributing the variation of its yield to the differences in temperature history.

Figure 10 shows several characteristic times for the pyrolysis process. The 50% and 95% point for evolution of measured

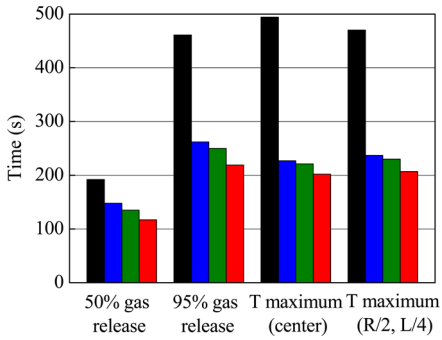

Figure 10. Characteristic times of gas release and of the occurrence of maximum temperature, for four different wood treatments: black: distilled water; blue: low KCl; green: high KCl; red: K_2CO_3.

gases were interpolated from the species histories for each wood treatment. Note that the time scale for tar production is believed to be similar to that for gas production, as both products are derived from the same feedstock materials, and thus the depletion of the feedstocks marks the end of the devolatilization process for both gases and tars. The other characteristic times were based on the positions of maxima of temperature at the two measurement locations.

The key observation from Figure 10 is that changing the kinetics through potassium doping has a substantial effect on all the characteristic pyrolysis times. Using each measure, the pyrolysis times of the water-washed samples are the longest, followed in order of decreasing pyrolysis time by the low-KCl, high-KCl, and K_2CO_3 samples. The ratio of slowest to fastest pyrolysis time varies from 1.6 to 2.45, depending on which measure is chosen, and in most cases the water-treated sample's time is much longer than the other three samples' times. The differences in conversion time appear to contradict the very low values of both internal and external pyrolysis numbers (Py),

DOI: 10.1021/acs.energyfuels.5b01776
Energy Fuels 2015, 29, 7350−7357

both estimated to be below 0.01 on the basis of cellulose kinetics evaluated at the external temperature. Note that similarly low values of Py were estimated by Bruch and Peters[33] for pyrolysis centimeter-scale wood particles at this temperature. On the basis of the low Py numbers, it was expected that changes in kinetics would have minimal effects on conversion times, because heat transfer was the limiting process. The samples studied here have essentially identical heat transfer characteristics but different kinetics.

This discrepancy exposes the difficulties of describing the pyrolysis process, especially on the centimeter scale, with values of a few dimensionless numbers. Most importantly, the use of the external temperature for evaluating the kinetic rate is not reasonable in the current experiment. 50% gas evolution occurred when the centerline temperature was only 242−309 °C and when the more relevant temperature at $L/4$, $R/2$ was at 357−371 °C. These temperatures, substantially below the external temperature of 427 °C, allow a greater role for kinetics in determining the devolatilization time scale. Thermochemistry appears to play an important role in ensuring that substantial fractions of the mass loss process occur at low temperatures: once endothermic pyrolysis processes start, they reduce the rate of temperature rise of the sample. Furthermore, the different kinetics of different important reactions may lead to very different values of Py depending on which reaction is selected.[34] It is clear that in this regime, pyrolysis time is determined by the interplay between heat transfer and chemistry.

Figure 10 also shows that the exothermic temperature excursion occurs near the end of the devolatilization process. This finding is in agreement with previous observations with for undoped solid wood particles[21,24,33] but not with observations for undoped packed beds.[21]

Finally, the form of the potassium and the potassium mass fraction, in the range tested, have relatively minor effects on characteristic times; the main difference is between the water-treated samples and the potassium-treated ones, as seen in the TGA results. The insensitivity of temperature histories, species yields, and characteristic times to the level of potassium present in the range of the doped samples, suggests that the nonuniformity of the potassium distribution in our samples may not have affected results significantly.

CONCLUSIONS

Here we present what we believe are the first measurements of the effect of potassium doping on centimeter-scale wood particles. These measurements are relevant to the behavior of engineering devices (e.g., updraft gasifiers or chip combustors), where biomass chips undergo thermal processes. Kinetically controlled submillimeter-scale TGA measurements, with externally imposed temperatures, are provided for comparison.

In the TGA experiments, potassium addition accelerated mass loss at a given temperature and tended to merge the peaks attributed to hemicellulose and lignin. Char yields increased with potassium addition at both centimeter and submillimeter scales.

The strong accelerating effect of potassium on the pyrolysis process was present at the centimeter-scale as well, even though pyrolysis occurred in the thermally thick regime. The pyrolysis of the centimeter-scale particles yielded information about the thermochemistry of the different stages of the pyrolysis process. For the milder cases of potassium catalysis, two exothermic processes separated by an endothermic process could be observed, in a pattern and in temperature ranges similar to those observed previously for undoped wood. Thus, although the kinetics were faster than for the water-treated sample, the thermochemistry appeared qualitatively similar. At higher dopant loading and for the more effective catalyst (K_2CO_3), the processes appeared to merge, but the observations were hindered by the cracking or splitting of the wood samples. Species histories for centimeter-scale particles showed large change in the timing of gas and volatile evolution, as well as distinct increase in yields for certain species and decreases for others with potassium addition. Spatially resolved modeling is needed to gain a better understanding of the interactions between thermochemistry, kinetics, and transport in the potassium-doped system.

Biomass materials naturally contain potassium and other catalytic materials at a variety of mass fractions. The present study indicates that the potassium level can have a strong effect on the pyrolysis time for these materials, even when they are pyrolyzed at the centimeter scale.

ASSOCIATED CONTENT

Supporting Information

The Supporting Information is available free of charge on the ACS Publications website at DOI: 10.1021/acs.energyfuels.5b01776.

Mineral content of biomass samples (PDF)

AUTHOR INFORMATION

Corresponding Author

*E-mail: emf4@cornell.edu. Tel.: 607-255-8309. Fax: 607-255-1222.

Present Address

[‖]LSU School of the Coast and Environment, Energy, Coast & Environment Building, Louisiana State University, Baton Rouge, LA 70803, United States

Notes

The authors declare no competing financial interest.

ACKNOWLEDGMENTS

The authors gratefully acknowledge the financial support of Yossie Hollander and Fondation des Fondateurs, as well as the State Scholarship Fund of China Scholarship Council. This work made use of the Cornell Center for Materials Research Facilities supported by the National Science Foundation under Award Number DMR-1120296. The authors thank Dr. Anthony Condo, Mr. Akio Enders, Mr. Dana Paul, Dr. Michael Rutzke, Prof. William B. Smith of SUNY ESF, and Ms. Colette Trouillot.

REFERENCES

(1) Vassilev, S. V.; Baxter, D.; Andersen, L. K.; Vassileva, C. G. *Fuel* **2010**, *89*, 913−933.

(2) Baxter, L. L.; Miles, T. R.; Miles, T. R., Jr.; Jenkins, B. M.; Milne, T.; Dayton, D.; Bryers, R. W.; Oden, L. L. *Fuel Process. Technol.* **1998**, *54*, 47−78.

(3) Nowakowski, D. J.; Jones, J. M.; Brydson, R. M. D.; Ross, A. B. *Fuel* **2007**, *86*, 2389−2402.

(4) Raveendran, K.; Ganesh, A.; Khilar, K. C. *Fuel* **1995**, *74*, 1812−1822.

(5) Fahmi, R.; Bridgwater, A. V.; Darvell, L. I.; Jones, J. M.; Yates, N.; Thain, S.; Donnison, I. S. *Fuel* **2007**, *86*, 1560−1569.

(6) Fahmi, R.; Bridgwater, A. V.; Donnison, I.; Yates, N.; Jones, J. M. *Fuel* **2008**, *87*, 1230−1240.

DOI: 10.1021/acs.energyfuels.5b01776
Energy Fuels 2015, 29, 7350−7357

(7) Oasmaa, A.; Solantausta, Y.; Arpiainen, V.; Kuoppala, E.; Sipila, K. *Energy Fuels* **2010**, *24*, 1380−1388.
(8) Yoshida, T.; Turn, S. Q.; Yost, R. S.; Antal, M. J. *Ind. Eng. Chem. Res.* **2008**, *47*, 9882−9888.
(9) Morgan, T. J.; Turn, S. Q.; George, A. *PLoS One* **2015**, *10*, e0136511.
(10) Mourant, D.; Wang, Z.; He, M.; Wang, X. S.; Garcia-Perez, M.; Ling, K.; Li, C. Z. *Fuel* **2011**, *90*, 2915−2922.
(11) Trendewicz, A.; Evans, R.; Dutta, A.; Sykes, R.; Carpenter, D.; Braun, R. *Biomass Bioenergy* **2015**, *74*, 15−25.
(12) Patwardhan, P. R.; Satrio, J. A.; Brown, R. C.; Shanks, B. H. *Bioresour. Technol.* **2010**, *101*, 4646−4655.
(13) Muller-Hagedorn, M.; Bockhorn, H.; Krebs, L.; Muller, U. *J. Anal. Appl. Pyrolysis* **2003**, *68*−*69*, 231−249.
(14) Di Blasi, C.; Galgano, A.; Branca, C. *Ind. Eng. Chem. Res.* **2009**, *48*, 3359−3369.
(15) Eom, I. Y.; Kim, J. Y.; Kim, T. S.; Lee, S. M.; Choi, D.; Choi, I. G.; Choi, J. W. *Bioresour. Technol.* **2012**, *104*, 687−694.
(16) Hwang, H.; Oh, S.; Cho, T. S.; Choi, I. G.; Choi, J. W. *Bioresour. Technol.* **2013**, *150*, 359−366.
(17) Yang, H.; Yan, R.; Chen, H.; Zheng, C.; Lee, D. H.; Liang, D. T. *Combust. Flame* **2006**, *146*, 605−611.
(18) Deng, L.; Zhang, T.; Che, D. *Fuel Process. Technol.* **2013**, *106*, 712−720.
(19) Wang, Z.; Wang, F.; Cao, J.; Wang. *Fuel Process. Technol.* **2010**, *91*, 942−950.
(20) Richards, G. N.; Zheng, G. *J. Anal. Appl. Pyrolysis* **1991**, *21*, 133−146.
(21) Di Blasi, C.; Branca, C.; Lombardi, V.; Ciappa, P.; Di Giacomo, C. *Energy Fuels* **2013**, *27*, 6781−6791.
(22) Corbetta, M.; Frassoldati, A.; Bennadji, H.; Smith, K.; Serapiglia, M.; Gauthier, G.; Melkior, T.; Ranzi, E.; Fisher, E. M. *Energy Fuels* **2014**, *28*, 3884−3898.
(23) Peters, B.; Bruch, C. *J. Anal. Appl. Pyrolysis* **2003**, *70*, 233−250.
(24) Bennadji, H.; Smith, K.; Shabangu, S.; Fisher, E. M. *Energy Fuels* **2013**, *27*, 1453−1459.
(25) Suleiman, B. M.; Larfeldt, J.; Leckner, B.; Gustavsson, M. *Wood Sci. Technol.* **1999**, *33*, 465−473.
(26) White, C. M.; Strazisar, B. R.; Granite, E. J.; Hoffman, J. S.; Pennline, H. W. *J. Air Waste Manage. Assoc.* **2003**, *53*, 645−715.
(27) ECN, 2015. *Phyllis2, database for biomass and waste*. Energy research Centre of the Netherlands. https://www.ecn.nl/phyllis2 (accessed July 26, 2015).
(28) Smith, D. N. R.; Cockcroft, R. *Nature* **1961**, *189*, 163−164.
(29) Di Blasi, C.; Galgano, A.; Branca, C. *Energy Fuels* **2009**, *23*, 1045−1054.
(30) Liu, Q.; Wang, S.; Luo, Z.; Cen, K. *J. Chem. Eng. Jpn.* **2008**, *41*, 1133−1142.
(31) Yang, H.; Yan, R.; Chen, H.; Zheng, C.; Lee, D. H.; Liang, D. T. *Energy Fuels* **2006**, *20*, 388−393.
(32) Yang, H. P.; Chen, H. P.; Du, S. L.; Chen, Y. Q.; Wang, X. H.; Zhang, S. H. *MRS Online Proc. Libr.* **2009**, *29*, 70−75 (in Chinese).
(33) Park, W. C.; Atreya, A.; Baum, H. *Combust. Flame* **2010**, *157*, 481−494.
(34) Gauthier, G.; Melkior, T.; Grateau, M.; Thiery, S.; Salvador, S. *J. Anal. Appl. Pyrolysis* **2013**, *104*, 521−530.
(35) Anca-Couce, A.; Mehrabian, R.; Scharler, R.; Obernberger, I. *Energy Convers. Manage.* **2014**, *87*, 687−696.
(36) Bennadji, H.; Smith, K.; Serapiglia, M.; Fisher, E. M. *Energy Fuels* **2014**, *28*, 7527−7537.

DOI: 10.1021/acs.energyfuels.5b01776
Energy Fuels 2015, 29, 7350−7357